

## MHD Flow in a U-bend of Circular Cross-section

Mistrangelo C.<sup>1\*</sup>, Bühler L.<sup>1</sup>

<sup>1</sup>Karlsruhe Institute of Technology, P.O. Box 3640, 76021 Karlsruhe, Germany.

\*Corresponding author: chiara.mistrangelo@kit.edu

**Abstract:** Liquid metal flow through a circular pipe forming a U-bend is investigated numerically for a constant Reynolds number, when a uniform magnetic field is imposed. The influence of the intensity of the applied magnetic field on flow structure, pressure and electric current distribution is studied via 3D numerical simulations. It is found that when the magnetic field is weak, a spiral motion develops that is fed by the fluid moving in the boundary layers. By increasing the magnetic field, the stronger electromagnetic forces weaken the vortical flow and significantly affect flow features leading to the formation of an internal fluid layer along the inner side of the bend, which carries most of the flow.

**Key words:** U-bend, pipe flow, secondary flow, magnetic field effects

**1. Introduction** Curved pipes are essential components in many technical applications such as heat exchangers, nuclear reactors, industrial piping systems and combustion engines. Hydrodynamic flows in bends are characterized by the occurrence of secondary motions in the form of two counter-rotating vortices known as Dean cells [1]. They are caused by a radial pressure gradient resulting from the centrifugal force acting on the fluid in the curved pipe section and their presence leads to increased mass and momentum transfer, and enhanced cross-sectional mixing. The secondary motion is affected by different parameters such as the curvature ratio and the Reynolds number [2]. Fully developed hydrodynamic flows in curved pipes have been extensively studied both numerically and experimentally [3]. Those analyses considered the characterization of Dean vortices, their stability, developing and turbulent flows [4]. On the other hand, the investigation of the influence of an externally imposed magnetic field on the flow in curved pipes did not receive much attention in the past [5]. In the present paper, we study numerically the magnetohydrodynamic (MHD) flow in an electrically conducting U-bend with circular cross-section when exposed to a uniform transverse magnetic field in the plane of the bend.

**2. Definition of the problem and mathematical model** We consider the viscous, incompressible, MHD flow of the liquid metal PbLi in the geometry shown in Figure 1a. It features two pipes of circular cross-section connected by a 180° bend, referred to as U-bend. The wall is electrically conducting with a thickness  $t_w = 3\text{mm}$ , and the axial lengths  $l_{xin}$  and  $l_{xout}$  of the inlet and outlet straight pipes have been selected depending on flow parameters. The former one is chosen such that the flow in the inlet duct reaches fully developed conditions before entering the bend. The latter one is long enough that all vortical structures shed in the turning part have been damped out before the flow reaches the exit of the pipe. Figure 1b shows details of the mesh employed for the solution of the problem. The mesh in the pipe cross-section is characterized by a uniform structured core region (1) and wall-parallel prism layers (2) closer to the solid domain. An additional uniform structured zone (3) for the transition between the

mesh portions 1 and 2 leads to better convergence. The various structured grids are joined by thin unstructured layers (4).

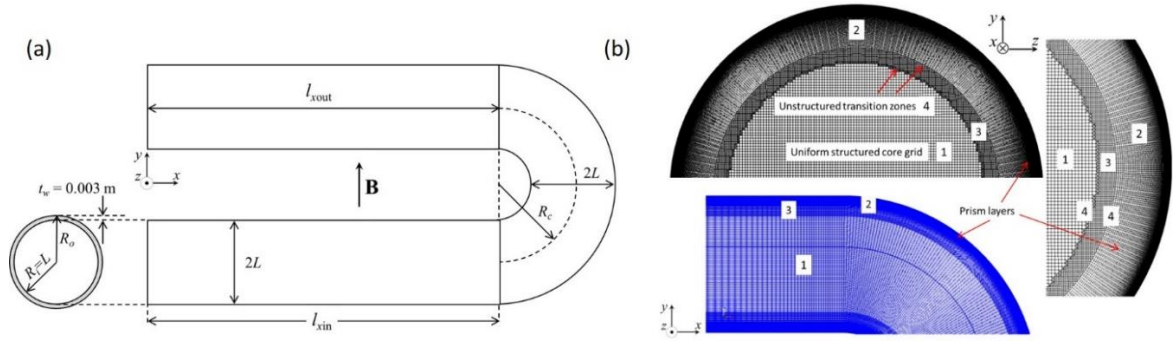


**Figure 1** Flow in a U-bend of circular cross-section with diameter  $2L$  and centreline curvature  $R_c$ . (a). Details of mesh used for the simulations (b).

The investigated liquid metal MHD flow is mathematically described by the momentum equation in which the electromagnetic Lorentz force appears as a source term. The electric current density is calculated via Ohm's law and driven by the gradient of the electric potential  $\phi$  and the induced electric field  $\mathbf{v} \times \mathbf{B}$ :

$$N^{-1} (\partial_t + \mathbf{v} \cdot \nabla) \mathbf{v} = -\nabla p + Ha^{-2} \nabla^2 \mathbf{v} + \mathbf{j} \times \mathbf{B}, \quad \text{and} \quad \mathbf{j} = -\nabla \phi + \mathbf{v} \times \mathbf{B}.$$

Conservation of mass  $\nabla \cdot \mathbf{v} = 0$  is satisfied by the solution of a pressure equation and a Poisson equation for the electric potential  $\nabla^2 \phi = \nabla \cdot (\mathbf{v} \times \mathbf{B})$  ensures conservation of charge  $\nabla \cdot \mathbf{j} = 0$ .

In the equations above,  $\mathbf{v}$ ,  $\mathbf{B}$ ,  $\mathbf{j}$ ,  $p$  and  $\phi$  stand for velocity, magnetic flux density, current density, pressure and electric potential, scaled by the reference quantities  $u_0$ ,  $B_0$ ,  $\sigma u_0 B_0$ ,  $\sigma u_0 B_0^2 L$  and  $u_0 B_0 L$ , respectively. The characteristic velocity  $u_0$  is the average velocity in the pipe,  $B_0$  the magnitude of the applied magnetic flux density, and  $L = R_i = 3.25\text{cm}$  is the typical length scale of the problem, chosen as the inner radius of the pipe. The fluid properties such as the electric conductivity  $\sigma$ , the kinematic viscosity  $\nu$ , and the density  $\rho$  are taken at a reference temperature of  $305^\circ\text{C}$  from reference [6].

The flow is characterized by two non-dimensional parameters, the Hartmann number  $Ha$  and the interaction parameter  $N$ :

$$Ha = B_0 L \sqrt{\frac{\sigma}{\rho \nu}}, \quad N = \frac{\sigma L B_0^2}{\rho u_0},$$

where  $Ha^2$  and  $N$  denote the ratios of electromagnetic to viscous and inertia forces, respectively. As alternative control parameter, we can introduce the Reynolds number  $Re = Ha^2 / N$  that describes the relative importance of inertia and viscous forces. The relative conductance of the wall with conductivity  $\sigma_w$  compared to the conductance of the fluid region is quantified by the wall conductance parameter  $c$  ([7], see Figure 1):

$$c = \frac{\sigma_w (R_o^2 - R_i^2)}{\sigma (R_o^2 + R_i^2)}.$$

As entrance condition, a fully developed MHD flow is applied with  $u_0$  as mean value. At the fluid-wall interface no-slip,  $\mathbf{v}=0$ , is imposed and it is assumed that no contact resistance is present such that electric potential and wall-normal current density are continuous,  $\phi = \phi_w$  and  $j_n = j_{nw}$ . The pressure at the outlet of the pipe is fixed at a reference value  $p_{\text{out}}=0$ .

**3. Results** In the following, results are discussed for the flow in a U-bend in the plane of the applied magnetic field  $\mathbf{B} = B_0 \hat{y}$ , with curvature ratio  $r = L/R_c = 0.5417$ , defined as the pipe radius  $L$  divided by the bend radius of curvature  $R_c$ ,  $c = 0.1175$ ,  $Re = 1000$  and different Hartmann numbers  $Ha$ .

Figure 2 shows the magnitude of the velocity on the symmetry plane at  $z = 0$  and on the  $xz$  middle-plane of the curved pipe for various Hartmann numbers  $Ha$ . The outlet pipe is much longer in the simulations and has been cut only for representation purposes. At  $Ha = 5$ , the flow resembles the hydrodynamic one ( $Ha = 0$ ) described in [2] in which, when approaching the bend, the inlet parabolic profile becomes asymmetric and its maximum shifts toward the internal wall of the pipe. Close to the turn, the fluid in the boundary layers starts describing spiral motions when moving upwards along the bend. On the horizontal  $xz$  plane, we recognise some typical features of hydrodynamic flow, such as the formation of a secondary flow pattern consisting in Dean-type cells, a separation cell near the inner wall (I) of the bend, and one appearing near the pipe centre (C).

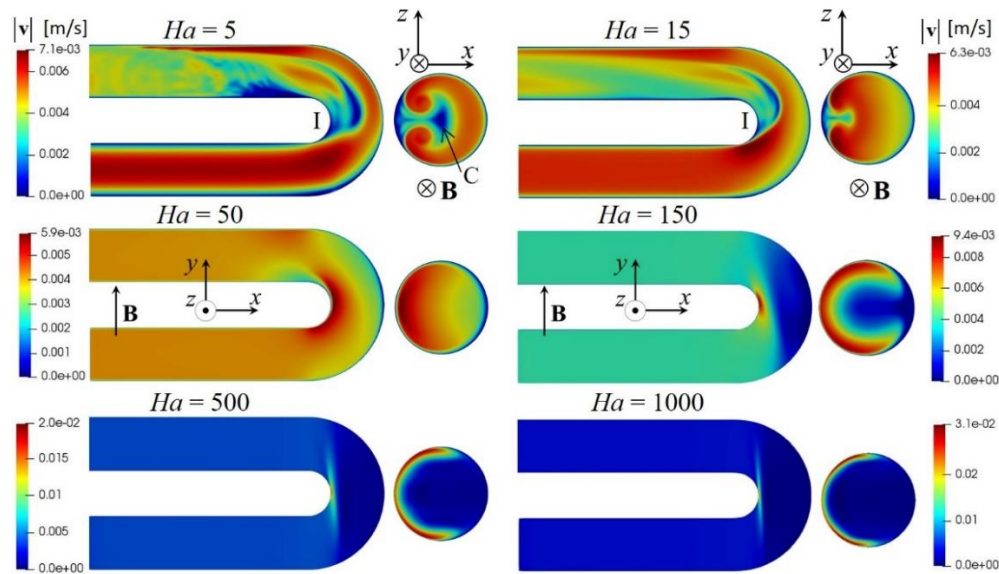


**Figure 2** Velocity magnitude on the symmetry plane  $z = 0$  and on the  $xz$  mid-plane for different Hartmann numbers  $Ha$ .

When increasing the strength of the magnetic field (see e.g.  $Ha = 15$ ) the stronger electromagnetic forces tend to stabilize the flow, weakening the spiralling flow structures. As a result, the front cell near I shrinks and the low-velocity zone in the centre C of the U-bend disappears. For more intense magnetic fields, an internal layer, which carries a large portion of the flow rate, develops tangent to the internal wall of the U-bend and becomes more and more aligned with magnetic field lines (see  $Ha = 1000$ ).

Three-dimensional velocity profiles are plotted in Figure 3 at different positions indicated by the centreline coordinate  $s$  of the curved pipe. At  $s = s_1$ , the MHD flow is fully developed with uniform core velocity and slight rise in the Roberts boundary layers that form where the magnetic field is parallel and tangent to the pipe wall [8]. At  $s = s_2$ , close to the bend, the velocity distribution is distorted compared to the fully developed profile with the maximum shifted towards the inner wall of the pipe. At  $s = s_3$ , on a plane inclined at an angle of  $45^\circ$  with the  $y$ -axis, a velocity jet starts developing in the boundary layer along the inner wall of the bend, while towards the outer wall there is almost no flow.

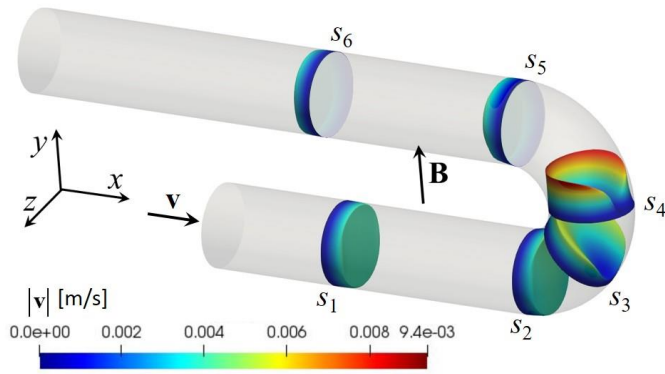


**Figure 3** Flow at  $Ha = 150$ . Three dimensional velocity profiles. The coordinate  $s$  varies along the pipe centreline.

In the centre of the bend at  $s = s_4$ , the velocity in the jet increases further. Behind the turn, after passing  $s_5$ , the flow recovers gradually a uniform fully developed profile (see  $s = s_6$ ).

In Figure 4 coloured contours of electric potential are plotted on the fluid-solid interface of the geometry (a) and typical current paths are illustrated via both a 3D and a top view of the U-bend (b).

It can be observed that in a certain portion of the inlet and outlet straight pipes (region 1), the potential is constant along magnetic field lines with variations in the transverse  $z$ -direction, as expected in fully developed MHD flows. Here near the side walls at  $z/L=\pm 1$ , the normalized electric potential  $\phi/\phi_0$  ( $z/L=\pm 1$ ) =  $\pm 0.8903$  is in accordance with estimates for fully developed pipe flow in electrically conducting pipes where  $(\phi/\phi_0)_{\text{FDF}}$  ( $z/L=\pm 1$ ) =  $\pm (1+c)^{-1} = \pm 0.8948$  [7]. In this zone (1), electric currents close through the walls in 2D cross-sectional planes (green paths). By approaching the turn (2), the electric potential reduces and it is no longer constant along magnetic field lines and it varies along the centreline direction  $s$ . The resulting electric potential gradient drives additional axial currents so that current loops arch in streamwise direction (blue and cyan current streamlines). In Figure 4b the top ( $xz$ ) view clearly shows the progressive build-up of an axial current component when moving closer to the turn. In the bend (3), complex 3D current loops occur, which close exclusively in the fluid without entering the wall (orange, black, red paths).

As observed in Figure 2 for flows at  $Ha = 500, 1000$ , when the intensity of the magnetic field increases, the main gradients of flow variables are confined in a layer that develops aligned to  $\mathbf{B}$  lines, along the internal wall of the curved pipe. As a result, also the current tends to flow in this boundary region, as visible in Figure 4c where contours of  $j_y$  are depicted on the cross-stream mid-plane of the bend for two  $Ha$ .

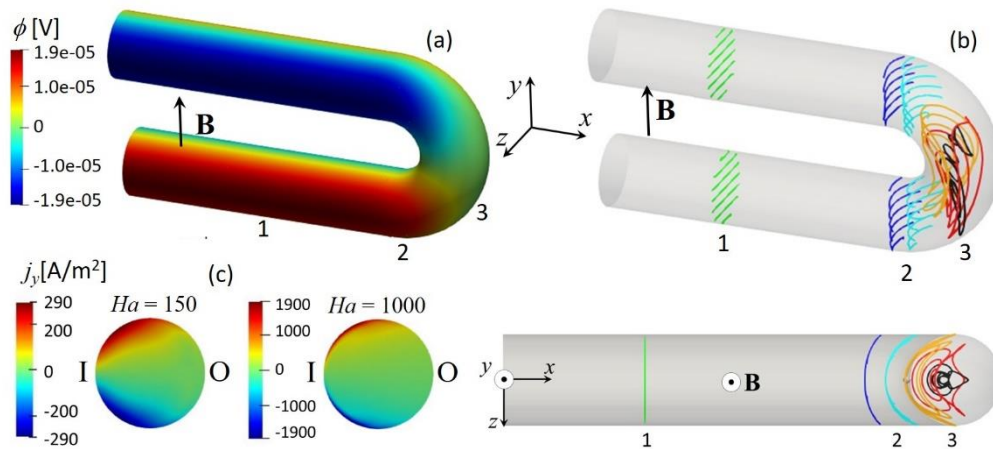


**Figure 4** Flow at  $Ha = 150$ . (a) Electric potential on the fluid-wall interface; (b) electric current paths: upstream and downstream, at a certain distance from the turn, the current closes its path in 2D cross-sectional planes (region 1). When approaching the bend (2), the axial potential gradient drives additional axial currents. In the bend, complex 3D current loops are present (3). (c) Contours of  $y$ -component of electric current in the  $xz$  middle plane: comparison between flows at  $Ha=150$  and  $Ha=1000$ .

As observed in Figure 2 for flows at  $Ha = 500, 1000$ , when the intensity of the magnetic field increases, the main gradients of flow variables are confined in a layer that develops aligned to  $\mathbf{B}$  lines, along the internal wall of the curved pipe. As a result, also the current tends to flow in this boundary region, as visible in Figure 4c where contours of  $j_y$  are depicted on the cross-stream mid-plane of the bend for two  $Ha$ .



The interaction of these 3D currents with the imposed magnetic field gives rise to Lorentz forces whose action modifies locally the pressure distribution. In Figure 5 the pressure scaled by  $p_0$  is plotted as a function of the normalized coordinate  $s/L$ , which varies along the U-bend, both at the centreline ( $z/L=0$ ) and near the side wall ( $z/L=1$ ) for 4 different Hartmann numbers  $Ha$ . The red dashed line indicates for strong magnetic fields the pressure gradient in fully developed pipe flow according to Miyazaki et al. [7], where  $\partial p/\partial x = -k_p \sigma u_0 B_0^2$  with  $k_p = c/(c+1)$ .

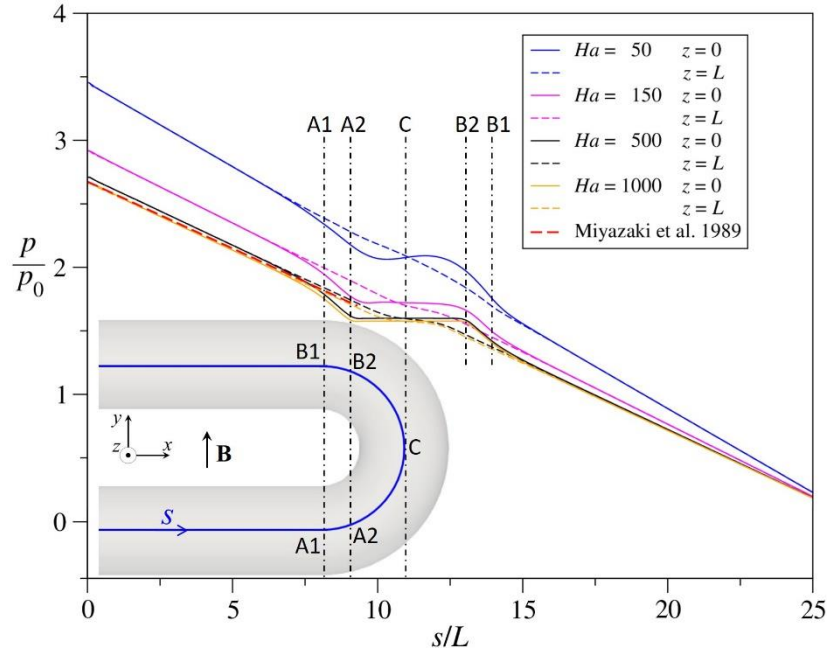


**Figure 5** Flow at  $Re = 1000$  and different  $Ha$ . Distribution of non-dimensional pressure along the central line of the U-bend ( $z/L = 0$ ) and near the side wall ( $z/L = 1$ ). The dashed red line indicates the pressure variation of the fully developed MHD flow in a pipe according to the formulation of Miyazaki et al. [7].

Close to the bend, the electromagnetic Lorentz forces generated by the 3D currents change the pressure distribution compared to the one in a fully developed pipe flow. When entering the turn (A1), the pressure in the vertical symmetry plane  $z/L=0$  starts decreasing faster than in an analogous fully developed flow. For sufficiently strong magnetic field, the pressure becomes almost constant between A2 and B2. After crossing the internal layer near B2 the pressure gradient approaches gradually the one of the fully developed pipe flow, as in the entrance pipe. Near the sides at  $z/L=1$ , where more intense transverse Lorentz forces compensate the pressure gradients, 3D effects are weaker than in the centre of the geometry. When  $Ha$  is large enough (e.g.  $Ha=500,1000$ ), the pressure gradient in the straight pipes is in very good agreement with the one predicted for fully developed flow [7].

**3. Conclusions** Numerical simulations have been carried out to study the liquid metal MHD flow in a circular pipe that forms a U-bend in the plane of the magnetic field. The influence of the strength of the imposed magnetic field on velocity and pressure distribution has been investigated. When the fluid enters the turn, axial currents are induced, which create Lorentz forces that modify the pipe flow compared to fully developed conditions. The secondary flow present at small  $Ha$  in the form of Dean-type vortices is suppressed when the magnetic field is increased. At sufficiently large  $Ha$ , the flow in the bend is characterized by the formation of a thin fluid layer aligned with  $\mathbf{B}$  lines and along the internal wall of the turn that carries most of the flow.

**Acknowledgments** This work has been carried out within the framework of the EUROfusion Consortium, funded by the European Union via the Euratom Research and Training Programme (Grant Agreement No 101052200 — EUROfusion). Views and opinions expressed are however those of the author(s) only and do not necessarily reflect those of the European Union or the European Commission. Neither the European Union nor the European Commission can be held responsible for them.

## References

- [1] W. R. Dean, “Note on the motion of fluid in a curved pipe,” *Philosophical magazine and Journal of Science*, vol. 4, pp. 208-223, 1927.
- [2] R. M. C. So, H. S. Zhang and Y. G. Lai, “Secondary cells and separation in developing laminar curved-pipe flows,” *Theoret. Comput. Fluid Dynamics*, vol. 3, pp. 141-162, 1991.
- [3] S. A. Berger, L. Talbot and L. S. Yao, “Flow in Curved Pipes,” *Annual Review of Fluid Mechanics*, vol. 15, no. 1, pp. 461-512, 1983.
- [4] A. Vester, R. Örlü and P. Alfredsson, “Turbulent flows in curved pipes: recent advances in experiments, simulations and analysis,” *Applied Mechanics Reviews*, vol. 68, 07 2016.
- [5] M. Hoque and M. Alam, “Effects of Dean number and curvature on fluid flow through a curved with magnetic field,” *Procedia Engineering*, vol. 56, pp. 245-253, 2013.
- [6] D. Martelli, A. Venturini and M. Utili, "Literature review of lead-lithium thermophysical properties," *Fusion Engineering and Design*, vol. 138, pp. 183-195, 2019.
- [7] K. Miyazaki, S. Inoue and N. Yamaoka, “MHD Pressure Drop of Liquid Metal Flow in Circular and Rectangular Ducts under Transverse Magnetic Field,” in *Liquid Metal Magnetohydrodynamics*, J. Lielpeteris and R. Moreau, Eds., Kluwer, 1989, pp. 29-36.
- [8] S. Vantighem, X. Albets-Chico and B. Knaepen, “The velocity profile of laminar MHD flows in circular conducting pipes,” *Theoretical and Computational Fluid Dynamics*, vol. 23, no. 6, pp. 525-533, 2009.